

OPTIMISING THE GEOMETRIC PARAMETERS OF A GEAR IN A TRACTOR TRANSMISSION UNDER CONSTRAINTS USING KISSOFT

Emre CAN^{*✉}, Mehmet BOZCA^{**✉}

^{*}Graduate School of Science and Engineering, Yildiz Technical University, Yildiz, 34349 Istanbul, Turkey

^{**}Mechanical Engineering Faculty, Machine Design Division, Yildiz Technical University, Yildiz, 34349 Istanbul, Turkey

canemreacan@hotmail.com, mbozca@yildiz.edu.tr

received 15 July 2022, revised 29 October 2022, accepted 13 November 2022

Abstract: We optimise the speed gears in a tractor transmission with KISSsoft software under three constraints: input power torque, transmission system volume and the gear ratio for each speed. This study aimed to optimise the module, face width, gear quality, centre distance, number of teeth, helix angle, addendum modification coefficient and pressure angle for each speed while considering the above constraints based on an optimisation chart. Tooth bending stress, tooth contact stress, contact ratio and specific sliding were considered during optimisation. Additionally, the effects of changes in a module on the gear profiles, overlap ratio, number of teeth and weight of the gear pair were examined. Strength calculations of gear pairs that were optimised and defined for all geometric parameters with KISSsoft were calculated with the mathematical model described in ISO 6336, and results were then compared. Finally, backlash was minimised for all gear pairs as defined with geometric parameters, and all dimensions and tolerances were determined for gear inspection after manufacturing. A concept design was also presented. We conclude that both the KISSsoft results and mathematical model results are within the range of the target value.

Key words: gears, geometric parameters, optimisation, KISSsoft

1. INTRODUCTION

Gears are typically used in many mechanical systems, particularly automotive systems, and can be designed to be more reliable, lighter and quieter via optimisation studies. Additionally, gears can be more cost-competitive during optimisation. Thus, many studies have investigated the optimisation of gears' geometric parameters.

Within the scope of the study, the results obtained with the mathematical model are compared with the results found with KISSsoft. In this study, both the mathematical model and KISSsoft analyses are carried out. This is the main difference that distinguishes this study from the existing studies in the literature.

The design and contact stress of helical gears in lightweight cars have been analysed in various studies. High stresses that cause pitting decrease as gear width increases. Contact failure in gears can be predicted by calculating contact stress [1].

The combined effects of the gear ratio, helix angle, face width and module on the bending and compressive stress of steel alloy helical gears have also been investigated. Increasing the module, face width and helix angle results in decreased tooth-root stress [2].

The effect of gear design variables on the dynamic stress of multistage gears has also been analysed. Increasing the module results in higher dynamic stress, increasing the pressure angle markedly increases stress levels, and increasing the contact ratio increases bending stress [3].

The effects of the module and pressure angle on contact stresses in spur gears have also been investigated. Studies have shown a decrease in contact fatigue life with an increase in the

module and pressure angle [4].

The effect of backlash on bending stresses in spur gears has also been investigated. Both stresses and deformations increase as a result of increased backlash [5].

The effects of gear parameters on the surface durability of gear flanks have also been investigated. The optimum parameters of cylindrical gear pairs are determined in terms of specific sliding and the contact stresses on the flanks [6].

The effects of sliding speed and specific sliding of the interval meshing gears have also been analysed. Increasing the profile shift coefficient decreases specific sliding but also decreases the contact ratio [7].

The effects of profile shifts in helical gear mechanisms with analytical and numerical methods have also been investigated. Both tooth-root stress and tooth contact stress decrease with a positive profile shift coefficient [8].

The optimisation of addendum modification for the bending strength of involute spur gears has also been studied. Increasing both the profile shift coefficient and pressure angle decreases tooth-root stress [9].

Finite element analysis of the contact stress and bending stress in the helical gear pair has also been performed. Increasing the helix angle increases both tooth-root stress and tooth contact stress [10].

The optimisation of the geometric parameters of gears under variable loading conditions has also been performed and show that tooth-root stresses increase due to negative profile shifts and decrease by positive profile shifts [11].

Effective design parameters have been optimised for an automotive transmission gearbox to reduce tooth bending stress. Both tooth-root stress and tooth contact stress decrease with

decreasing contact ratio via an increasing pressure angle [12].

Empirical model-based optimisation of gearbox geometric design parameters to reduce rattle noise in an automotive transmission was presented and showed that by optimising the geometric parameters of the gearbox, it is possible to obtain a lightweight gearbox structure and minimise rattling noise [13].

Torsional vibration model-based optimisation of gearbox geometric design parameters to reduce rattle noise in an automotive transmission was studied and showed that by optimising the geometric parameters of the gearbox, it is possible to obtain a lightweight gearbox structure and minimise rattling noise [14].

Transmission error model-based optimisation of the geometric design parameters of an automotive transmission gearbox to reduce gear-rattle noise showed that by optimising the geometric parameters of the gearbox, it is possible to obtain a gear structure with high bending and contact strengths, and to minimise the torsional vibration, transmission error and gear-rattling noise [15].

The remainder of the present study is structured as follows: Section 2 discusses the calculation of the load-carrying capacity of the helical gear; Section 3 the optimisation concept; Section 4 the optimisation steps with KISSsoft; Section 5 provides the results and discussion; and Section 6 presents the conclusions.

2. CALCULATING THE LOAD CAPACITY OF HELICAL GEARS

Gears encounter tooth bending stress and tooth contact stress during power-torque transfers. Therefore, damage can occur on gears due to stresses on the gears, which must be considered during design.

2.1. Tooth bending stress

The tangential force creates a bending stress on the tooth, and the radial force creates a compressive stress on the tooth. These forces cause stress concentrations at the root of the tooth, and the stress concentration must be considered so that the load capacity of the gear can be calculated. The distribution of the forces on the gears is shown in Fig. 1, and the tooth bending stress according to the ISO 6336 standard is calculated as follows [16]:

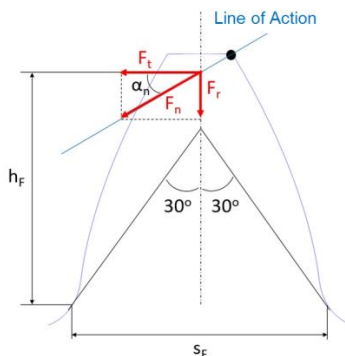


Fig. 1. Tooth bending stress

The real tooth-root stress, σ_F , is calculated as follows:

$$\sigma_F = \frac{F_t}{b m_n} Y_F Y_S Y_\epsilon Y_\beta K_A K_V K_{F\beta} K_{F\alpha} \quad (1)$$

where F_t is the nominal tangential load (N), b is the face width (mm), m_n is the normal module (mm), Y_F is the form factor (-), Y_S is the stress correction factor (-), Y_ϵ is the contact ratio factor (-), Y_β is the helix angle factor (-), K_A is the application factor (-), K_V is the dynamic factor (-), $K_{F\beta}$ is the face load factor (-) and $K_{F\alpha}$ is the transverse load factor (-).

The permissible bending stress, σ_{FP} , is calculated as follows:

$$\sigma_{FP} = \sigma_{F \lim} Y_{ST} Y_N Y_\delta Y_R Y_X \quad (2)$$

where $\sigma_{F \lim}$ is the nominal stress (N/mm²), Y_{ST} is the stress correction factor (-), Y_N is the life factor (-), Y_δ is the relative notch sensitivity factor (-), Y_R is the relative surface factor (-) and Y_X is the size factor (-).

The safety factor for bending stress S_F is calculated as follows:

$$S_F = \frac{\sigma_{FP}}{\sigma_F} \quad (3)$$

2.2. Tooth contact stress

The force that affects the surfaces in contact with each other in the gear pair creates a high surface pressure called Hertzian contact stress shown in Fig.2 due to the effect on a small area of the surface during power transmission. These stresses cause wear and pitting depending on material fatigue. The surface pressure that occurs on gears is calculated according to the ISO 6336 standard as follows [17]:

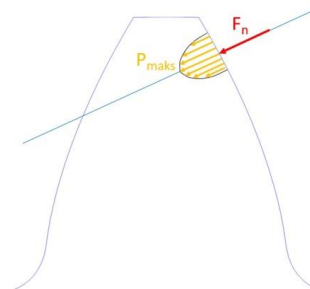


Fig. 2. Tooth contact stress

The real contact stress, σ_H , is calculated as follows:

$$\sigma_H = \sqrt{\frac{F_t(u+1)}{b m_n u}} Z_H Z_E Z_\epsilon Z_\beta \sqrt{K_A K_V K_{H\beta} K_{H\alpha}} \quad (4)$$

where u is the gear ratio (-), Z_H is the zone factor (-), Z_E is the elasticity factor, Z_ϵ is the contact ratio factor (-), Z_β is the helix angle factor (-), $K_{H\beta}$ is the face load factor and $K_{H\alpha}$ is the transverse load factor (-).

The permissible contact stress, σ_{HP} , is calculated as follows:

$$\sigma_{HP} = \sigma_{H \lim} Z_N Z_L Z_V Z_R Z_W Z_X \quad (5)$$

where $\sigma_{H \lim}$ is the allowable stress (N/mm²), Z_N is the life factor (-), Z_L is the lubrication factor (-), Z_V is the velocity factor (-), Z_R is the roughness factor (-), Z_W is the work hardening factor (-) and Z_X is the size factor (-).

The safety factor for contact stress, S_H , is calculated as follows:

$$S_H = \frac{\sigma_{HP}}{\sigma_H} \quad (6)$$

3. OPTIMISATION

Gears are currently used in many mechanical systems. Both safe and cheaper gear systems can be designed via optimisation, and efficient systems can be created to determine requisite geometric parameters. During optimisation, all geometric parameters of the gear pairs are determined step by step, as indicated in the flow chart below:

1. Face width, gear quality and first-level module optimisation
2. Outputs: the module graphic, S_F , S_H ; changes in the gear profiles; the overlap ratio; the teeth number; the gear ratio; and the system weight
3. Centre-distance optimization
4. Outputs: the tip-diameter graphic; the centre distance; and the S_F , S_H , centre-distance graphic
5. Last-level module optimisation
6. Number of teeth optimisation
7. Outputs: the specific-sliding graphic, the number of teeth, and the contact ratio
8. Helix angle optimisation
9. Outputs: axial forces and contact ratio
10. Addendum modification coefficient optimisation
11. Outputs: the angle-of-rotation graphic, the specific sliding and changes in the gear profiles
12. Pressure-angle optimisation
13. Comparison of the results for both the KISSsoft and mathematical models
14. Outputs: tooth bending stress, tooth contact stress and safety factors
15. Backlash optimisation
16. Outputs: dimensions and tolerances for inspection of all gears after manufacturing
17. Concept design
18. Outputs: conceptual 3D design

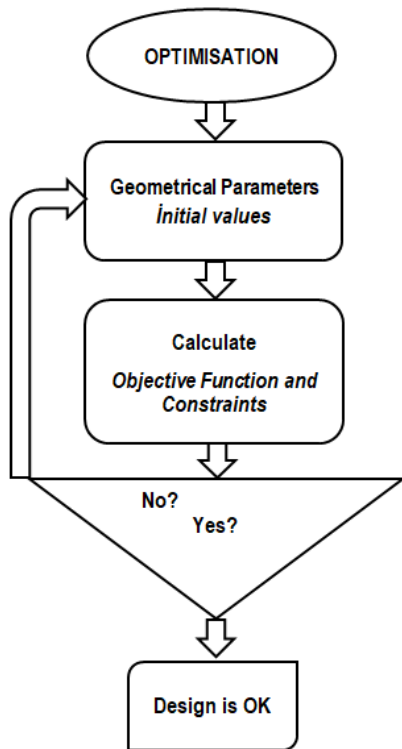


Fig. 3. Flow chart of optimisation

4. OPTIMISATION WITH KISSSOFT

Four speed gears of a tractor transmission shown in Fig.4 were optimised via KISSsoft software in this study. The input power was 50 kW, and the torque was 238 Nm for the speed gears that were optimised in this study. These four speed gears have ratios that are similar to those in Tab. 1 with tolerances of 4%.

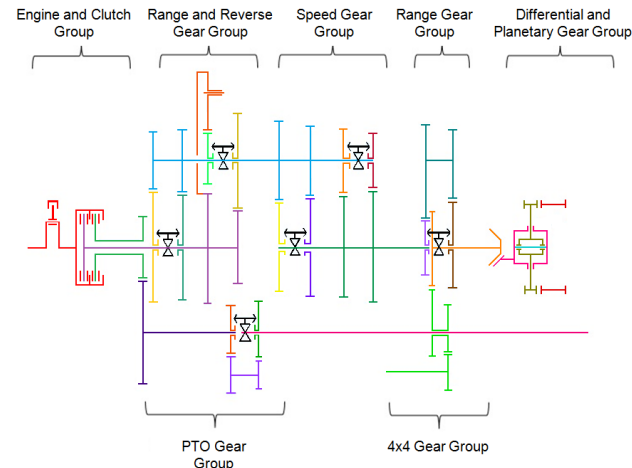


Fig. 4. Gear scheme of tractor transmission

Tab. 1. Ratios

Speed	Ratio (4%)
1	3.1
2	1.9
3	1.1
4	0.7

The volume that can be used for speed gears is limited due to other systems on both tractors and transmission. The maximum volume that can be used in transmission for these speed gear groups is shown in Fig. 5.

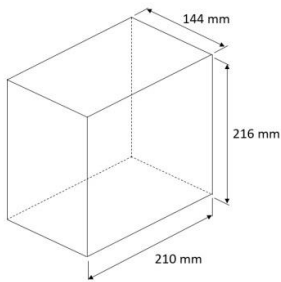


Fig. 5. Maximum volume

4.1. Gear width, gear quality and first-level module optimisation

First, suitable geometric parameters of gear width, gear quality and module were calculated while considering constraints with KISSsoft. Other geometric parameters were assumed to be constant, and these other geometric parameters were optimised in the subsequent steps to design an efficient system.

The vertical dimension was considered 186 mm (216– 30 mm) during optimisation because all gear pairs that assemble at the same centre distance can use space approximately 15 mm along the vertical dimension based on the number of teeth and module of gear pairs. The centre distance was considered 93 mm (186 mm/2 mm) during the first optimisation step so that two shafts could be placed at 186 mm. Volume measures are shown in Fig.6.

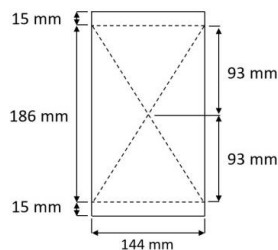


Fig. 6. Centre distance

The pressure angle was considered to be 20°, which is used as a standard for many manufacturers. The helix angle was considered to be 17°, which is the average value for similar tractor transmission. The material was defined as 16 MnCr5, which is used in similar systems. These parameters were accepted as specified initially but were later optimised.

First, optimisation was begun with the same gear width for four gear pairs, and then each gear width was defined according to the results. The horizontal dimension was 210 mm, as shown in Fig. 5 and Fig.7. Four gears (b_1 , b_2 , b_3 and b_4) and two synchroneshes (s_1 and s_3) must be placed 210 mm away from each other. Each synchronesh requires 50 mm in the horizontal direction, and there should be 5 mm spaces (s_2) between the second and third gears for safety due to production and assembly errors. The initial gears' widths are shown in Tab. 2.

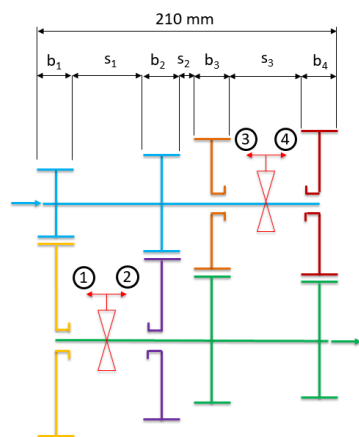


Fig. 7. Four speed gear group

Tab. 2. Gear widths

s_1 (mm)	s_2 (mm)	s_3 (mm)	b_1 (mm)	b_2 (mm)	b_3 (mm)	b_4 (mm)
50	5	50	26.25	26.25	26.25	26.25

Gear pairs that can be used for the first speed gear were calculated with KISSsoft considering 50 kW power, 238 Nm torque, 3.1 gear ratio, 20° pressure angle, 17° helix angle, 93 mm centre

distance, 7 quality, 26.25 mm gear width, and a module between 1 mm and 5 mm. According to the results, 386 different solutions were found for the first speed gear pair, and all results are shown in Fig. 8 to evaluate the parameters. In the figure, the horizontal axis represents the module, the vertical axis represents the minimum root safety and the colour scale represents the minimum flank safety. Increasing the module results appears to increase the root safety. For the 1 mm module, root safety was calculated to be approximately 0.6, for the 4.8 mm module, it was approximately 2.1. Considering the colour scale, the colours change from red to blue with increasing modules; thus, increasing the module results in decreased flank safety.

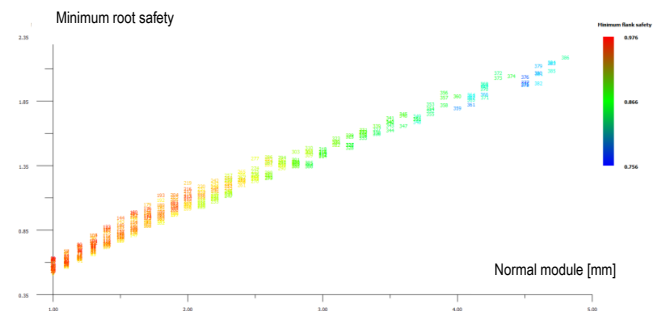


Fig. 8. Optimisation of the first speed gear pairs ($b = 26.25$ mm)

For this system, the root safety is between 1.3 and 1.5. There are some optimisation steps for this study; thus, root safeties that are between 1.1 and 1.9 are sufficient for this first optimisation considering that there can be changes in other steps. Additionally, the flank safeties must be at least 1, and average value of flank safety have to be 1.1 in the figure. According to Fig. 8, all flank safeties are <1 ; thus, these gear pairs cannot be used for this system. Gear width and quality were changed so that flank safeties could be increased. First, the gear width was increased to 35 mm and 40 mm, and then the gear quality was increased from 7 to 6. The gear width was not increased by >40 mm because the horizontal dimension was limited, and space is needed for other gear pairs. The results based on these new parameters are shown in Figs. 9–11 and Tab. 3.

Tab. 3. Optimisation of the first speed gear pairs with new parameters

Gear width (mm)	Gear quality	S_{Hmin}
26.25	7	0.756
35	7	0.919
40	7	0.982
40	6	1.018

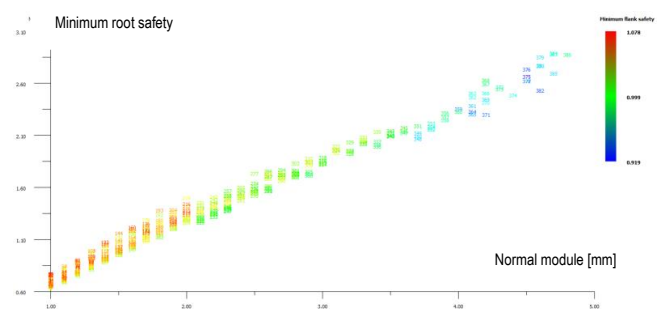


Fig. 9. Optimisation of the first speed gear pairs with new parameters ($b = 35$ mm)

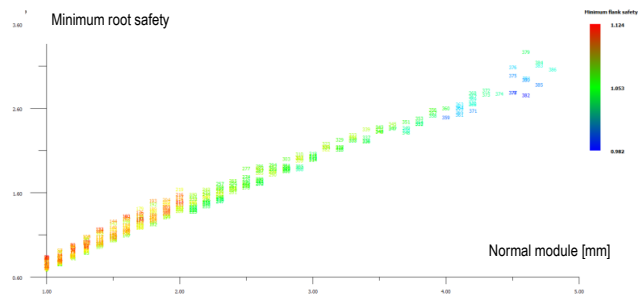


Fig. 10. Optimisation of the first speed gear pairs with new parameters ($b = 40$ mm, 7 quality)

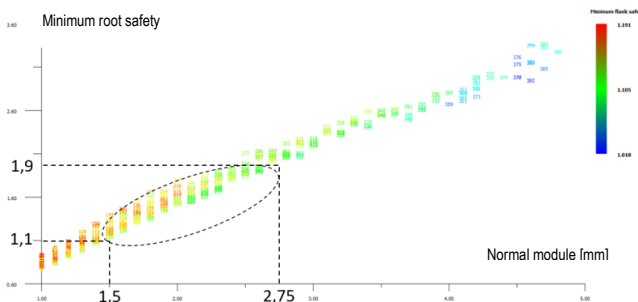


Fig. 11. Optimisation of the first speed gear pairs with new parameters ($b = 40$ mm, 6 quality)

According to the results, a 40 mm gear width and a quality of 6 yield the optimal first speed gear pair. Additionally, the module should be between 1.5 mm and 2.75 mm wide.

After optimising the first speed gear pairs, the second speed gear pairs were optimised. The input conditions were the same as in the first gear optimisation except for the ratio, which was set to 1.9. According to the results, 587 different solutions were found, and the results are shown in Tab. 4 and Fig. 12. According to the results, a 25 mm gear width and a quality of 7 yielded the optimal second speed gear pair. Additionally, the module should be between 1.5 mm and 2.75 mm wide.

Tab. 4. Optimisation of the second speed gear pairs with new parameters

Gear width (mm)	Gear quality	S_{Hmin}
30	7	1.130
25	7	1.016

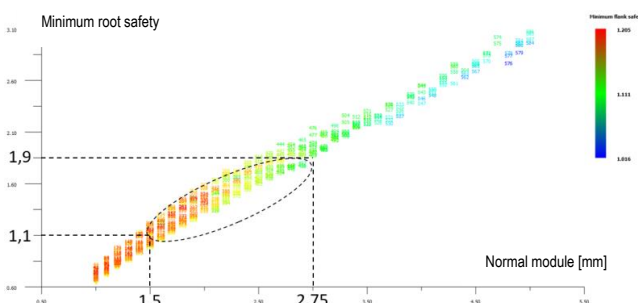


Fig. 12. Optimisation of the second speed gear pairs ($b = 25$ mm)

After optimisation of the first and second speed gear pairs, a 40 mm horizontal space remained as the horizontal limit of the

system. Therefore, the gear width was set equal to 20 mm for both the third and fourth speed gear pairs.

Optimisation was performed for the third speed gear pair, and 774 different solutions were found. As shown in Tab. 5 and Fig. 13, a 20 mm gear width and a quality of 8 yielded the optimal third speed gear pair. Additionally, the module should be between 1.5 mm and 3 mm.

Finally, the fourth speed gear pair was optimised, and 716 different solutions were found. As shown in Tab. 6 and Fig. 14, a 20 mm gear width and a quality of 8 yielded the optimal fourth speed gear pair. Additionally, the module should be between 1.5 mm and 2.75 mm.

Tab. 5. Optimisation of the third speed gear pairs with new parameters

Gear width (mm)	Gear quality	S_{Hmin}
20	7	1.063
20	8	1.009

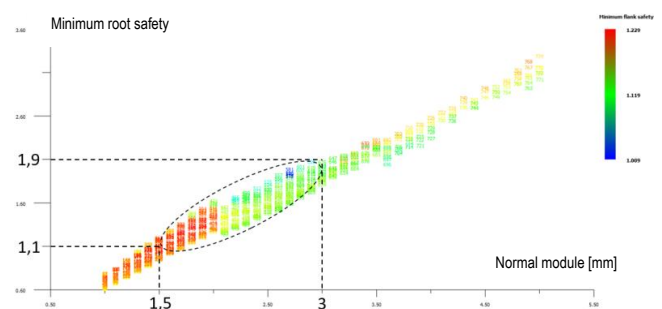


Fig. 13. Optimisation of the third speed gear pairs (8 quality)

Tab. 6. Optimisation of the fourth speed gear pairs with new parameters

Gear width (mm)	Gear quality	S_{Hmin}
20	7	1.186
20	8	1.111

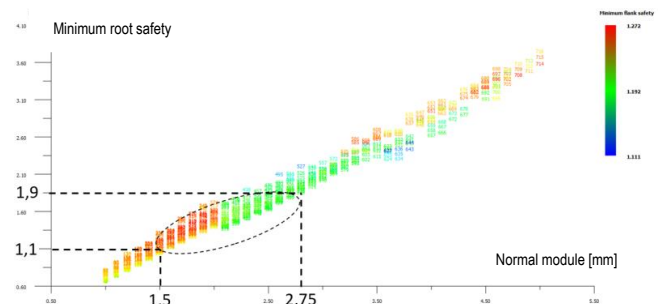


Fig. 14. Optimisation of the fourth speed gear pairs (8 quality)

4.2. Centre-distance optimisation

The centre distance was set equal to 93 mm, which is the centre of the useable vertical dimension of considering the gear width, quality and first-level module optimisation. In this step, the centre distance was optimised between reasonable values of 86 mm and 98 mm.

For the first speed gear pair, the optimisation was performed with the following assumptions: 50 kW power, 238 Nm torque, 3.1 gear ratio, 20° pressure angle, 17° helix angle, quality of 6, 40

gear width, and modules between 1.5 mm and 2.75 mm with standard measurements in steps of 0.25 mm. Based on these values, 1,006 different solutions were found. The tip diameters of gears are important to optimise the centre distance due to volume constraints. In Fig. 15, the horizontal axis represents the tip diameters of the driver gear, the vertical axis represents the tip diameters of the driven gear and the colour scale represents the centre distances.

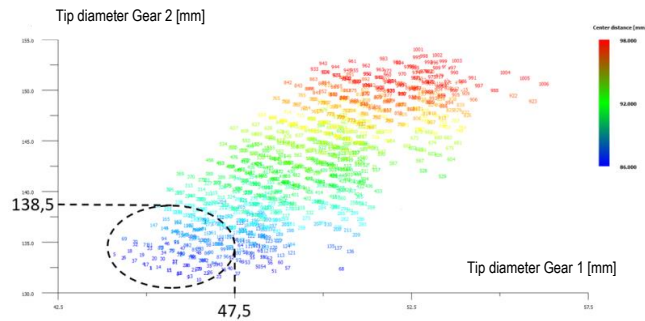


Fig. 15. Centre distance for the first speed gear pair

According to input constraints, the horizontal limit is 144 mm, and the vertical limit is 216 mm; thus, 186 mm is used due to assembly conditions. Additionally, 2 mm of space for each side of the gears was included; thus, the horizontal limit was considered to be 140 mm. Thus, the tip diameter of each gear should not be >140 mm. Additionally, the sum of the tip diameters of the gear pair should not be >186 mm. According to Fig. 15, the tip diameter of the driver gear can reach 47.5 mm, and the tip diameter of the driven gear can reach 138.5 mm when considering the two above-mentioned constraints. For these values, the solutions are shown in blue; thus, the centre distances between 86 mm and 90 mm are suitable for the first speed gear pair according to the colour scale.

Additionally, Fig. 16 was generated using the same solutions to optimise the centre distance for the case shown in Fig. 15. In the figure, the horizontal axis represents the centre distances, the vertical axis represents the flank safety of the gear pair and the colour scale represents the root safety of the gear pair. Increasing the centre distance is shown to increase the flank safety. Average flank safety must be approximately 1.1; however, the average flank safety is <1.1 for centre distances of 86 mm and 87 mm. Therefore, centre distances of 88 mm, 89 mm and 90 mm are suitable for the first speed gear pair based on Figs. 15 and 16.

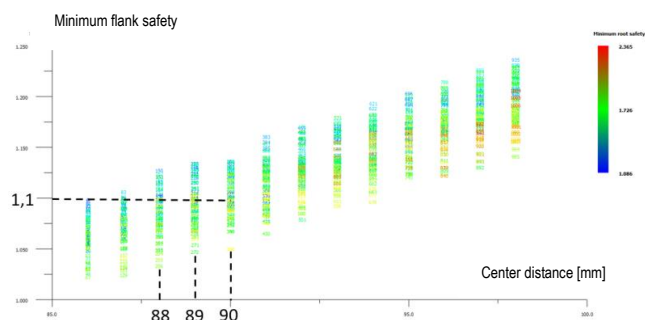


Fig. 16. Centre distance for the first speed gear pair

Then, optimisation was performed for the second speed gear pair, and 1,584 solutions were found according to the input constraints. Figs. 17 and 18 show that the tip diameter of the driver

gear can reach 65.5 mm, and the tip diameter of the driven gear can reach 120.5 mm. Additionally, centre distances between 86 mm and 89 mm are shown to be suitable.

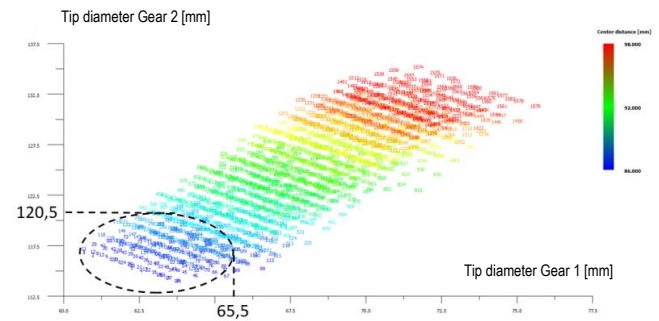


Fig. 17. Centre distance for the second gear pair

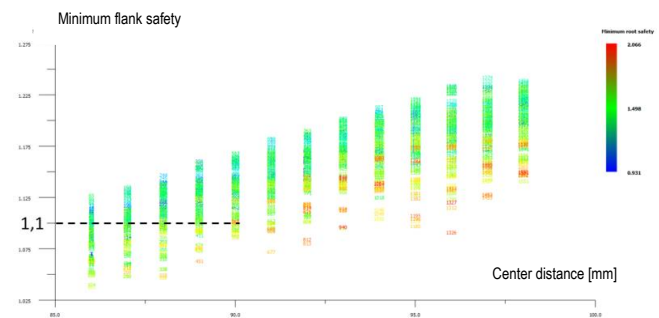


Fig. 18. Centre distance for the second gear pair

An optimisation of the third speed gear pair was then performed and yielded 2,265 solutions. As shown in Figs. 19 and 20, the tip diameter of the driver gear can reach 88 mm, and the tip diameter of the driven gear can reach 98 mm. A centre distance between 86 mm and 90 mm is shown to be suitable, and values >90 mm are overdesigned for this gear pair.

Finally, an optimisation was performed for the fourth speed gear pair, and 1,997 solutions were found. As shown in Figs. 21 and 22, the tip diameter of the driver gear can reach 107.5 mm, and the tip diameter of the driven gear can reach 78.5 mm. Additionally, all centre distances are suitable for the fourth speed gear pair, but other gear pairs must be considered during optimisation.

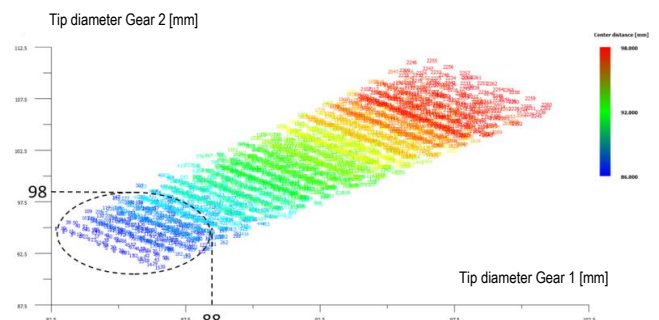


Fig. 19. Centre distance for the third gear pair

Results show that the centre distance can be between 88 mm and 90 mm when considering all gear pairs. Therefore, a centre distance of 89 mm was selected based on all of the optimisations performed.

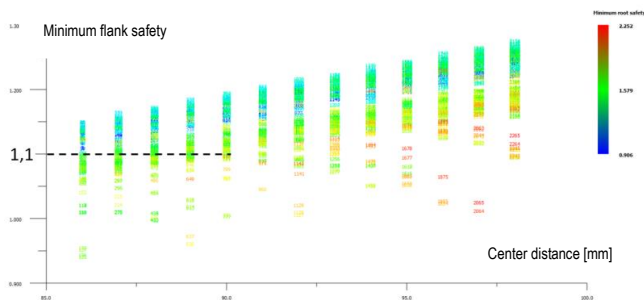


Fig. 20. Centre distance for the third gear pair

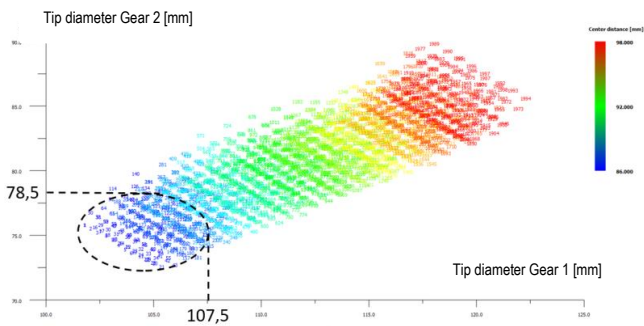


Fig. 21. Centre distance for the fourth speed gear pair

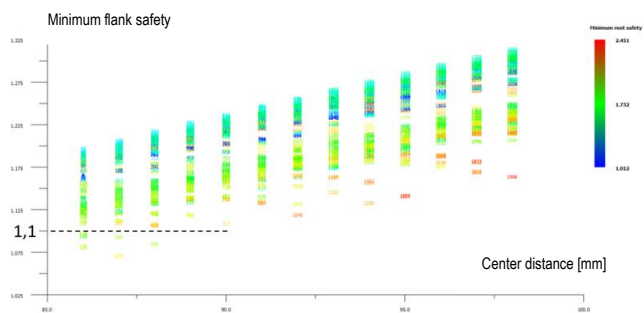


Fig. 22. Centre distance for the fourth speed gear pair

4.3. Last-level module optimisation

During the first-level module optimisation, the module was defined as a range for all speed gear pairs according to the results. A last-level module optimisation was then performed to determine certain modules.

This optimisation was performed for the first speed gear pair while considering the following input values: 50 kW power, 238 Nm torque, 3.1 gear ratio, 20° pressure angle, 17° helix angle, 89 mm centre distance, quality of 6, 40 mm gear width, and a module between 1.5 mm and 2.75 mm. With these inputs, 230 solutions were found. In Fig. 23, the horizontal axis represents the module, the vertical axis represents the root safety and the colour scale represents the flank safety.

The root safety must be between 1.3 and 1.5 for this last-level optimisation, and a 1.75 mm module yields a root safety between 1.3 and 1.5. However, according to previous experience from field tests, the durability of the first speed gear pair can be problematic due to the associated high gear ratio; therefore, a 2 mm module was used to increase safety. This situation is only valid for the first speed gear pair, and there is no need to overdesign the other speed gear pairs.

Then, an optimisation was performed for the second speed gear pair. According to calculations based on input constraints,

115 solutions were found and are shown in Fig. 24, where the root safety is between 1.3 and 1.5 with 2 mm modules.

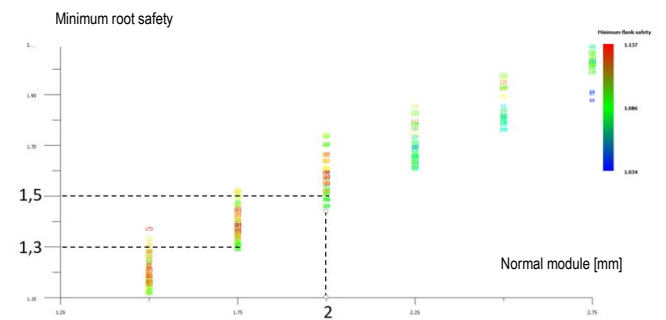


Fig. 23. Module optimisation for the first speed gear

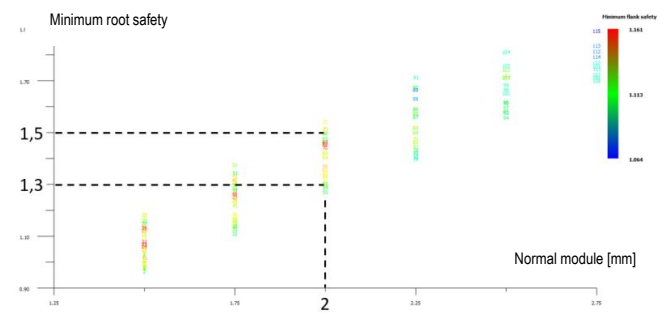


Fig. 24. Module optimisation for the second speed gear

Then, an optimisation was performed for the third speed gear pair, and 162 solutions were found, as indicated in Fig. 25. A 2 mm module is shown to be suitable for root safety, which is between 1.3 and 1.5.

Finally, an optimisation was performed for the fourth speed gear pair, and 162 solutions were found, as indicated in Fig. 26. A 1.75 mm module is shown to satisfy root-safety requirements, which is between 1.3 and 1.5.

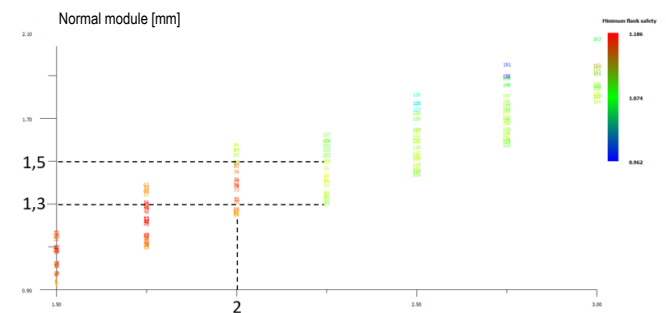


Fig. 25. Module optimisation for the third speed gear

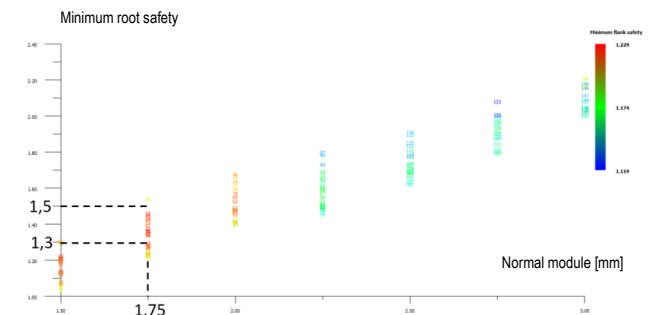


Fig. 26. Module optimisation for the fourth speed gear

4.4. Number of teeth optimisation

After optimising the gear width, gear quality, centre distance and module, the number of teeth of the gear pair that is suitable for the defined ratio must be determined. Therefore, an optimisation of the number of gear teeth was performed.

First, an optimisation was performed for the first speed gear pair with the following input values: 50 kW power, 238 Nm torque, 3.1 gear ratio, 20° pressure angle, 17° helix angle, 89 mm centre distance, gear quality of 6, 40 mm gear width and 2 mm module.

All gear pairs with defined ratios were calculated with KISSsoft. According to calculations, 14 different gear pairs were found, as shown in Tab. 7, which describes the number of teeth of driver gear (z_1), the number of teeth of driven gear (z_2), the profile shifts of driver gear (x_1), the profile shifts of driven gear (x_2), the total contact ratio (ϵ_y), the maximum specific sliding (ζ_{max}) and the gear ratio (i).

In Fig. 27, the horizontal axis represents the maximum specific sliding, the vertical axis represents the number of teeth of driver gear and the colour scale represents the total contact ratio.

The maximum specific sliding should be between -1 and $+1$ to avoid wear on the gears. In the figure, solutions 2, 3, 6 and 9 appear to meet the requirements of specific sliding. Additionally, solution 9 has the highest contact ratio according to the colour scale. The gear pair that has a high contact ratio does not produce much noise during meshing. Therefore, a high contact ratio is desirable for gear systems. According to the results, solution 9 can be used for the first gear pair. However, as shown in Tab. 7, solution 9 has 21 teeth for the driver gear and 63 teeth for the driven gear. In this case, the ratio is $63/21 = 3$, which causes wear on the teeth because the same teeth work during meshing. For this reason, solution 6 with a gear pair of 20–64 was preferred.

Tab. 7. Number of teeth optimised for the first speed gear pair

Sol. no.	z_1	z_2	x_1	x_2	ϵ_y	$\zeta_{maks.}$	i
1	20	63	0.31984	0.87368	3.215	-1.268	3.15
2	20	63	0.41984	0.77368	3.203	-1.04	3.15
3	20	63	0.51984	0.67368	3.189	-0.847	3.15
4	20	64	0.20295	0.40344	3.319	-1.619	3.2
5	20	64	0.30295	0.30344	3.304	-1.294	3.2
6	20	64	0.40295	0.20344	3.287	-1.031	3.2
7	21	63	0.1933	0.41309	3.325	-1.529	3
8	21	63	0.2933	0.31309	3.311	-1.237	3
9	21	63	0.3933	0.21309	3.295	-0.996	3
10	21	64	0.09127	-0.03291	3.417	-2.003	3.048
11	21	64	0.19127	-0.13291	3.4	-1.561	3.048
12	21	64	0.29127	-0.23291	3.381	-1.218	3.048
13	21	65	0.01277	-0.46034	3.496	-2.794	3.095
14	21	65	0.11277	-0.56034	3.472	-2.023	3.095

Then, an optimisation was performed for the second speed gear pair, and 21 solutions were found, as indicated in Fig. 28. According to Fig. 28, solution 18 with a gear pair of 30–55 is suitable in terms of both the specific sliding and total contact ratio.

Then, an optimisation was performed for the third speed gear pair, and 24 solutions were found, as indicated in Fig. 29. Solution 13 with a gear pair of 40–45 is optimal.

Finally, an optimisation was performed for the fourth speed gear pair, and 27 solutions were found, as indicated in Fig. 30.

According to the results, solution 20 with a gear pair of 57–41 is suitable in terms of specific sliding and the total contact ratio.

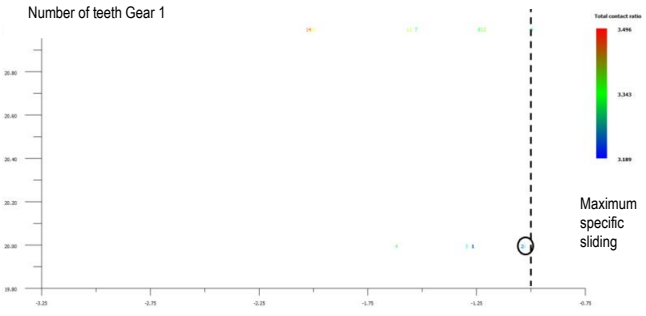


Fig. 27. Number of teeth optimised for the first speed gear pair

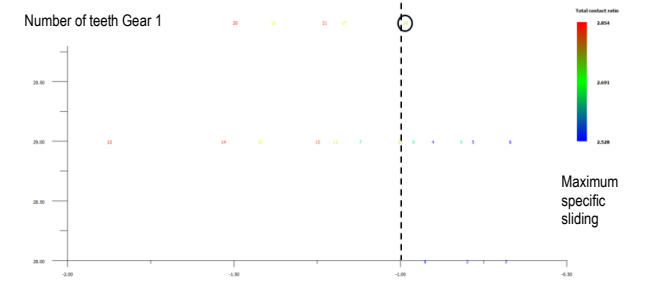


Fig. 28. Number of teeth optimised for the second speed gear pair

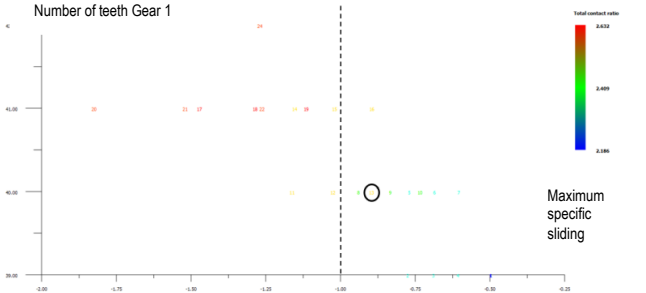


Fig. 29. Number of teeth optimised for the third speed gear pair

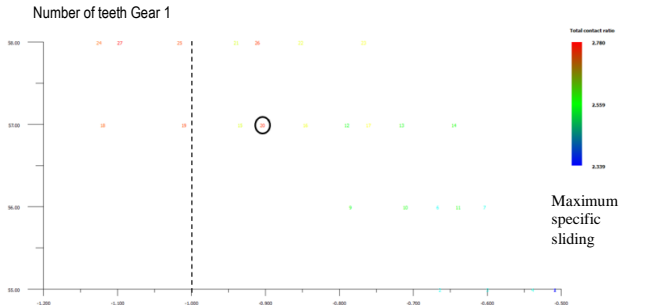


Fig. 30. Number of teeth optimisation for fourth speed gear pair

4.5. Helix angle optimisation

The helix angle of gear pairs was optimised after optimising the gear width, gear quality, module and number of teeth. Currently, the gear pair uses a helix angle so that it can operate quietly due to the high contact ratio. Although such a gear pair has an advantage in terms of the noise level, gear pairs with helix angles

generate axial forces on the systems as shown in Fig.31. Therefore, the helix angle is important for the design of shafts and bearings.

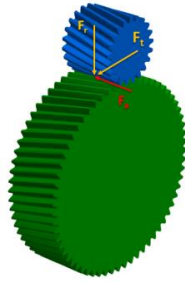


Fig. 31. Forces on gear

An optimisation of the helix angle for the first speed gear pair was performed while considering the following input values: 50 kW power, 238 Nm torque, 3.1 gear ratio, 20° pressure angle, 89 mm centre distance, quality of 6, 40 mm gear width, 2 mm module, and helix angles of 13°, 15°, 17° and 19°, which are geometrically satisfactory.

The calculated axial force and total contact ratio according to the helix angle are shown in Tab. 8. A higher contact ratio results in increased axial forces, and a high contact ratio tends to produce lower noise levels; however, a high axial force is not ideal for shaft and bearing systems.

For this system, a contact ratio of 2.5 appears minimal based on previous experience from field tests. According to Tab. 8, all helix angles have a contact ratio that is >2.5; thus, a 13° helix angle was selected for the first speed gear pair due to its minimal axial force.

Tab. 8. Helix angles for first speed gear pair

Helix angle β (°)	Axial force F_a (N)	Contact ratio (ϵ_y)
13	2,685.2	2.774
15	3,089.4	3.062
17	3,489.9	3.342
19	3,886.2	3.610

The results for the second speed gear pair are shown in Tab. 9, and a 15° helix angle was selected for the second speed gear pair due to its minimal helix angle, which yields a total contact ratio that is >2.5.

Tab. 9. Helix angle for second speed gear pair

Helix angle β (°)	Axial force F_a (N)	Contact ratio (ϵ_y)
13	1,790.1	2.364
15	2,059.6	2.566
17	2,326.6	2.759
19	2,590.8	2.934

The results for the third and fourth speed gear pairs are shown in Tabs. 10 and 11. A 17° helix angle for the third speed gear and a 15° helix angle for the fourth speed gear were selected based on the total contact ratio.

Tab. 10. Helix angles for third speed gear pair

Helix angle β (°)	Axial force F_a (N)	Contact ratio (ϵ_y)
13	1,342.6	2.170
15	1,544.7	2.358
17	1,745.0	2.536
19	1,943.1	2.694

Tab. 11. Helix angles for fourth gear pair

Helix angle β (°)	Axial force F_a (N)	Contact ratio (ϵ_y)
13	1,076.8	2.365
15	1,238.9	2.574
17	1,399.5	2.763

4.6. Addendum modification coefficient optimisation

An optimisation was then performed on the addendum modification coefficient, which can be determined based on the defined module, helix angle and centre distance.

First, an optimisation was performed for the first speed gear pair while considering the following inputs: 50 kW power, 238 Nm torque, 3.1 gear ratio, 20° pressure angle, 13° helix angle, 89 mm centre distance, quality of 6, 40 mm gear width, 2 mm module, and an addendum modification coefficient between 0 and +0.7 that is geometrically satisfactory. Results of this optimisation are shown in Tab. 12.

Tab. 12. Addendum modification coefficient for the first speed gear pair

x_1	0	0.1	0.2	0.3	0.4	0.5	0.6	0.7
x_2	1.54	1.44	1.34	1.24	1.14	1.04	0.94	0.84
ζ_{1min}	-2.52	-2.07	-1.70	-1.41	-1.16	-0.95	-0.78	-0.63
ζ_{1maks}	0.26	0.30	0.33	0.36	0.39	0.41	0.43	0.46
ζ_{2min}	-0.36	-0.43	-0.50	-0.57	-0.64	-0.71	-0.78	-0.85
ζ_{2maks}	0.71	0.67	0.63	0.58	0.53	0.48	0.43	0.38
ϵ_y	2.77	2.77	2.76	2.75	2.74	2.73	2.72	2.70
S_{F1}	1.32	1.35	1.38	1.40	1.42	1.43	1.44	1.45
S_{F2}	1.70	1.63	1.56	1.51	1.46	1.42	1.39	1.36
S_H	1.09	1.09	1.09	1.08	1.08	1.07	1.07	1.06

In Tab. 12, increasing the addendum modification of the driver gear from 0 to +0.7 results in a decrease in the addendum modification of the driver gear from 1.54 to 0.84 due to the constant centre distance. Increasing the addendum modification of the driver gear from 0 to +0.7 results in an increase in root safety from 1.32 to 1.45 due to an increase in tooth thickness. Additionally, decreasing the addendum modification of the driven gear results in decreasing root safety from 1.70 to 1.36 due to thinning of tooth thickness.

Increasing the addendum modification of the driver gear results in a decrease in the total contact ratio from 2.77 to 2.70. Additionally, this change has some effect on flank safety.

Increasing the addendum modification of the driver gear from 0 to +0.7 results in decreasing the specific sliding of the driver gear from 2.52 to -0.63 of the driver gear, increasing the specific sliding of the driven gear from -0.3 to -0.85. According to the results, an addendum modification of +0.6 should be used for this system. Additionally, Fig. 32 shows the associated specific sliding according to the angle of rotation of the gear. In the figure, A-B-C-

D-E represents the contact point of the gear pair during meshing, the red curve represents the driver gear and the green curve represents the driven gear.

Then, an optimisation was performed for the second speed gear pair, and the results are shown in Tab. 13 and Fig. 33. According to the results, an addendum modification coefficient of +0.3 for the driver gear is suitable.

Then, an optimisation was performed for the third speed gear pair, and the results are shown in Tab. 14 and Fig. 34. According to the results, an addendum modification coefficient of +0.1 for the driver gear is suitable.

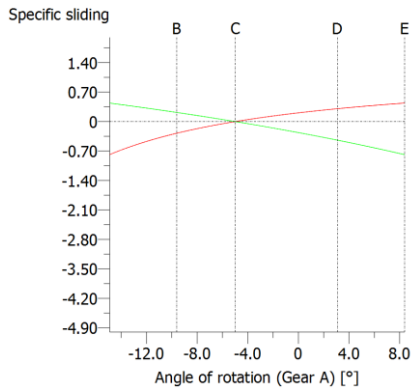


Fig. 32. Specific sliding of the first speed gear pair for +0.6 of the addendum modification coefficient of the driver gear

Tab. 13. Addendum modification coefficient for the second speed gear pair

x_1	-0.2	-0.1	0	0.1	0.2	0.3	0.4	0.5
x_2	0.72	0.62	0.52	0.42	0.32	0.22	0.12	0.02
ζ_{1min}	-1.83	-1.59	-1.37	-1.18	-1.01	-0.86	-0.72	-0.60
ζ_{1maks}	0.30	0.33	0.37	0.40	0.42	0.45	0.48	0.50
Z_{2min}	-0.43	-0.50	-0.58	-0.66	-0.75	-0.83	-0.92	-1.01
Z_{2maks}	0.64	0.61	0.57	0.54	0.50	0.46	0.42	0.37
ϵ_y	2.56	2.56	2.56	2.56	2.55	2.54	2.53	2.52
S_{F1}	1.24	1.27	1.29	1.31	1.33	1.34	1.34	1.35
S_{F2}	1.36	1.34	1.33	1.32	1.31	1.29	1.28	1.26
S_H	1.14	1.14	1.14	1.14	1.13	1.13	1.13	1.12

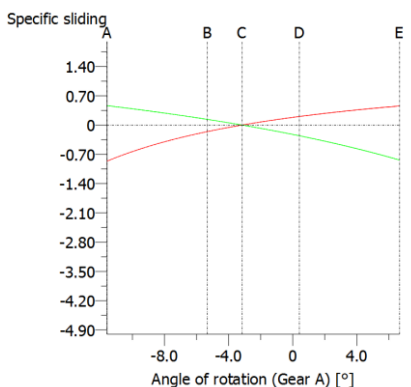


Fig. 33. Specific sliding of the second speed gear pair for +0.3 of addendum modification of the driver gear

Finally, an optimisation was performed for the fourth speed gear pair, and the results are shown in Tab. 15 and Fig. 35. According to the results, an addendum modification coefficient of +0.1 for the driver gear is suitable.

According to the results, an addendum modification coefficient of 0 for the driver gear is suitable.

Tab. 14. Addendum modification coefficient for the third speed gear pair

x_1	-0.2	-0.1	0	0.1	0.2	0.3
x_2	0.25	0.15	0.05	-0.04	-0.14	-0.24
ζ_{1min}	-1.24	-1.09	-0.96	-0.84	-0.72	-0.61
ζ_{1maks}	0.38	0.42	0.45	0.48	0.51	0.54
Z_{2min}	-0.63	-0.73	-0.83	-0.94	-1.06	-1.19
Z_{2maks}	0.55	0.52	0.49	0.45	0.42	0.38
ϵ_y	2.532	2.535	2.536	2.534	2.529	2.522
S_{F1}	1.273	1.294	1.311	1.324	1.333	1.338
S_{F2}	1.338	1.329	1.318	1.303	1.284	1.262
S_H	1.128	1.129	1.129	1.128	1.127	1.125

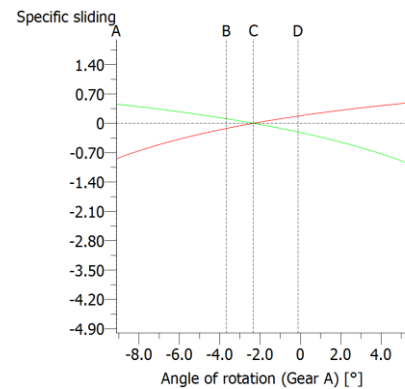


Fig. 34. Specific sliding of the third speed gear pair for +0.1 of addendum modification of the driver gear

Tab. 15. Addendum modification coefficient for the fourth speed gear pairs

x_1	-0.2	-0.1	0	0.1	0.2	0.3
x_2	0.32	0.22	0.12	0.02	-0.07	-0.17
ζ_{1min}	-0.96	-0.87	-0.78	-0.69	-0.61	-0.53
ζ_{1maks}	0.35	0.39	0.43	0.46	0.50	0.53
Z_{2min}	-0.56	-0.65	-0.76	-0.88	-1.00	-1.14
Z_{2maks}	0.49	0.46	0.43	0.41	0.38	0.34
ϵ_y	2.558	2.567	2.574	2.579	2.581	2.580
S_{F1}	1.284	1.300	1.315	1.327	1.339	1.350
S_{F2}	1.351	1.346	1.340	1.331	1.319	1.304
S_H	1.214	1.216	1.219	1.220	1.223	1.226

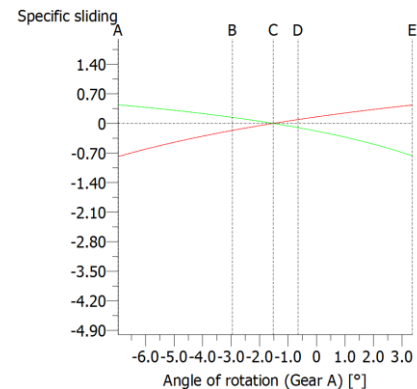


Fig. 35. Specific sliding of the fourth speed gear pair for +0.1 of addendum modification of the driver gear

4.7. Pressure-angle optimisation

After optimising other geometric parameters, pressure-angle optimisation was performed while considering pressure angles of 14° , 16° , 18° , 20° and 22° . Results are shown in Tab. 16.

Tab. 16. Pressure angles for the first speed gear pair

α_n	14°	16°	18°	20°	22°
x_1	0.6	0.6	0.6	0.6	0.6
x_2	1.0894	1.0236	0.9766	0.9419	0.9157
ζ_{1min}	-1.53	-1.19	-0.95	-0.78	-0.65
ζ_{1maks}	0.50	0.48	0.46	0.43	0.41
Z_{2min}	-1.00	-0.93	-0.86	-0.78	-0.71
Z_{2maks}	0.60	0.54	0.48	0.43	0.39
ϵ_y	2.784	2.772	2.750	2.724	2.697
S_{F1}	1.410	1.419	1.432	1.447	1.463
S_{F2}	1.367	1.363	1.373	1.391	1.412
S_H	1.017	1.038	1.055	1.070	1.082

Although the addendum modification of the driver gear was constant, the addendum modification of the driven gear changed due to changing the pressure angle from 14° to 22° . Increasing the pressure angle results in a decrease in the total contact ratio due to thinning of the top section of the gear.

Increasing the pressure angle results in increased root safety of the driver gear from 1,410 to 1,463 due to thickening of the tooth root.

Specific sliding was not limited at pressure angles of 14° and 16° but was at 18° , 20° and 22° . However, the difference among these values is small; therefore, a pressure angle of 20° was selected because it is a standard value that is used by most manufacturers. Additionally, the optimisation results are similar for other speed gear pairs, and a pressure angle of 20° was also selected for the other gear speed pairs.

4.8. Backlash optimisation

Backlash optimisation was performed after determining all geometric parameters of the gear pairs. Backlash occurs in gear pairs due to installation faults, gear quality and thermal expansion of the system. Therefore, some backlash is generated with tooth thickness tolerances and centre-distance tolerances. These two factors are optimised for suitable backlash.

After optimising the first speed gear pair, the tooth thicknesses of the gears are shown in Fig. 36.

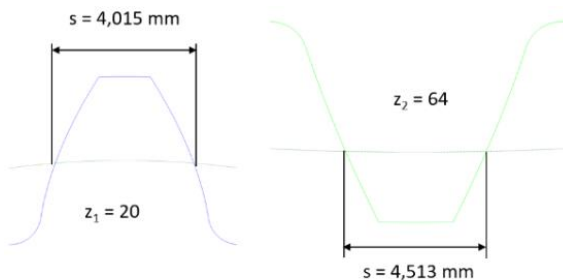


Fig. 36. Tooth thickness of first speed gear pair

There are different methods that are used by manufacturers to measure backlash. In this study, circumferential backlash is considered during optimisation as shown in Fig.37.

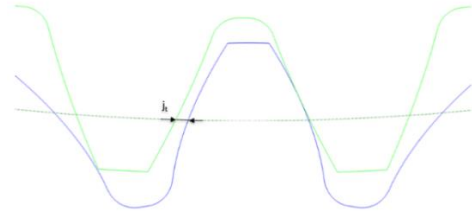


Fig. 37. Circumferential backlash

In this gear system, suitable backlash is considered to be between 0.1 mm and 0.3 mm based on practical experience. Therefore, tooth thickness tolerances and centre-distance tolerances are determined according to the considered backlash values. First, the backlash value is calculated while considering only the tooth thickness of the first speed gear pair; results are shown in Tab. 17. According to Tab. 17, backlash is suitable for tooth thickness tolerances between -0.05 mm and -0.14 mm.

Tab. 17. Backlash for first speed gear pair

Tolerance (mm)	Backlash (mm)
-0.03	0.064
-0.05	0.106
-0.08	0.170
-0.13	0.275
-0.14	0.297
-0.15	0.318

In addition to tooth thickness tolerances, centre-distance tolerances affect the backlash values. If gear pairs are near each other, backlash decreases, and if the gear pair's axes are more distant, backlash increases as shown in Fig.38. Centre-distance tolerances consist of the dimensional deviation of the shaft, bearing and casting.

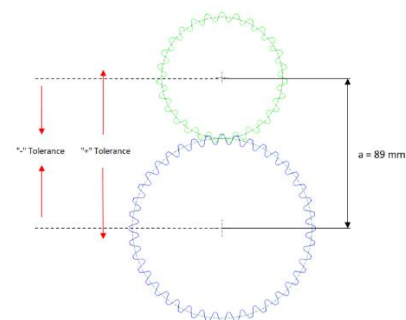


Fig. 38. Centre-distance tolerances

As shown in Tab. 18, backlash values were calculated considering the ISO 286 standard of centre-distance tolerances and tooth thickness tolerances between -0.05 mm and -0.14 mm. As mentioned before, suitable backlash is between 0.1 mm and 0.3 mm. According to Tab. 17, the backlash values are near the target for J6, J7 and J8 centre-distance tolerances. Additionally, the

backlash values are outside of the target for J9 and J10. Although the backlash is near the target for J6 and J7, these tolerance groups are not suitable in terms of manufacturing tractor parts. Therefore, the tolerances of J8 are selected for this system.

Tab. 18. Backlash for first speed gear pair

Standards	Positive (+) tolerance (mm)	Negative (−) tolerance (mm)	Min. backlash (mm)	Max. backlash (mm)
-	0	0	0.106	0.297
ISO 286 J6	+0.011	-0.011	0.096	0.307
ISO 286 J7	+0.0175	-0.0175	0.090	0.313
ISO 286 J8	+0.027	-0.027	0.081	0.322
ISO 286 J9	+0.0435	-0.0435	0.066	0.337
ISO 286 J10	+0.07	-0.07	0.041	0.362

Then, tooth thickness tolerances were calculated again considering ISO 286 J8 so that the backlash values are between 0.1 mm and 0.3 mm. Results are shown in Tab. 19. According to the results, −0.06 mm and −0.13 mm tolerances of tooth thickness are suitable for the first speed gear pairs.

The tolerances of other gear pairs and dimensions for inspection of all the gear pairs were calculated similarly and are shown in Tab. 19.

4.9. Optimisation results

The optimisation results for the four speed gear groups are shown in Tab. 19. Additionally, the dimensions and tolerances for inspection of all the gears are shown in Tab. 19.

The optimal four speed gears were placed in a volume, as shown in Fig. 39, which confirms that the design meets the volume constraint; all gears can be assembled properly in the volume.

Tab. 19. Optimisation results

Parameters	1. Speed	2. Speed	3. Speed	4. Speed
Number of teeth z_1	20	30	40	57
Number of teeth z_2	64	55	45	41
Module (mm)	2	2	2	1.75
Pressure angle (°)	20	20	20	20
Helix angle (°)	13	15	17	15
Addendum modification coefficient x_1	0.6	0.3	0.1	0
Addendum modification coefficient x_2	0.9419	0.2201	-0.0416	0.1297
Face width (mm)	40	25	20	20
Quality	6	7	8	8
Total weight (kg)	5.262	2.861	2.133	2.155

Tooth thickness of z_1 (mm)	3.885–3.955	3.448–3.518	3.157–3.227	2.619–2.689
Tooth thickness of z_2 (mm)	4.383–4.453	3.332–3.402	2.951–3.021	2.784–2.854
Base tangent length between k teeth of z_1	21.967–22.033 k: 4 teeth	27.785–27.851 k: 5 teeth	33.761–33.827 k: 6 teeth	35.001–35.066 k: 7 teeth
Base tangent length between k teeth of z_2	59.188–59.253 k: 10 teeth	46.162–46.227 k: 8 teeth	33.726–33.792 k: 6 teeth	29.557–29.623 k: 6 teeth
Dimension over balls/ball diameter of z_1	49.800–49.925 D: 4.250	68.655–68.807 D: 3.750	88.706–88.877 D: 3.500	107.068–107.249 D: 3.000
Dimension over balls/ball diameter of z_2	140.226–140.381 D: 3.750	119.340–119.512 D: 3.500	98.594–98.772 D: 3.500	78.472–78.644 D: 3.000
Centre distance (mm)	88.973–89.027			
Backlash (mm)	0.102–0.300	0.102–0.300	0.105–0.293	0.105–0.293

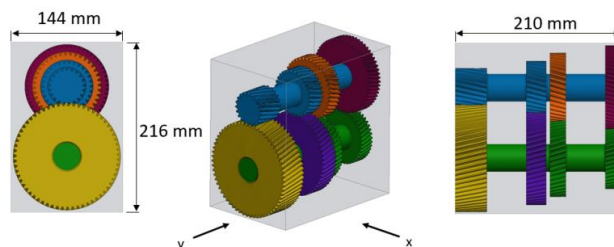


Fig. 39. Speed gears in a volume

5. RESULTS AND DISCUSSION

Many results and relations between geometric parameters of the gear pairs were observed during optimisation. These relations are important when designing efficient gear systems.

Changing the module was found to affect the root safety by changing the gear profiles, as shown in Fig. 40. Increasing the module has an effect on the tooth thickness and seriously affects root safety.

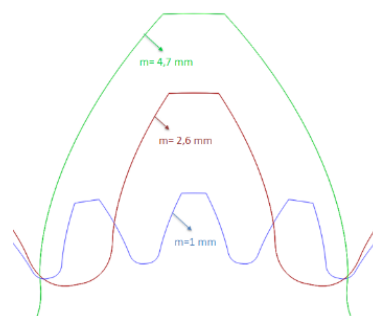


Fig. 40. Gear profiles based on the module

Apart from gear profiles, the module affects the overlap ratio, which also affects both the durability and noise level of the gear pairs. In Figs. 41–43, the contact pattern of the gear pairs is shown on the face width. Decreasing the module thus increases the overlap ratio due to the decreased size of the gear profiles.

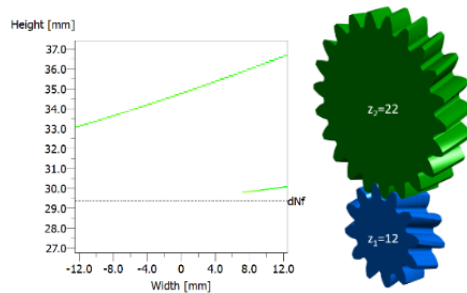


Fig. 41. Contact pattern ($m = 5$ mm, $i = 1.8$)

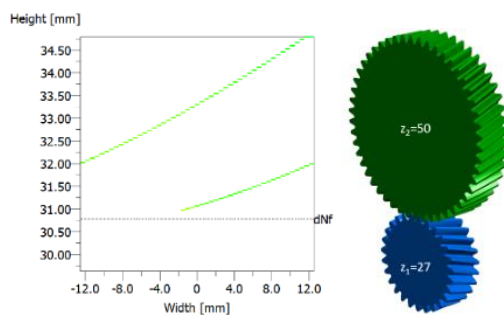


Fig. 42. Contact pattern ($m = 2.3$ mm, $i = 1.8$)

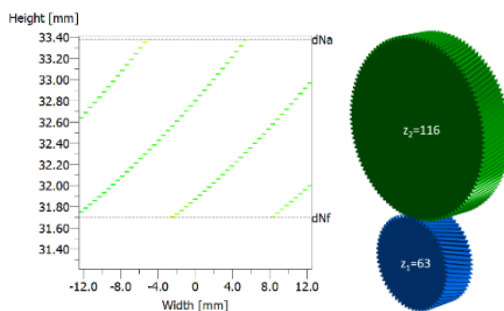


Fig. 43. Contact pattern ($m = 1$ mm, $i = 1.8$)

Finally, the module affects the weights of the gear pair, which is an important constraint for the systems. As shown in Fig. 44, increasing the module increases the weight for the same ratio of gear pairs.

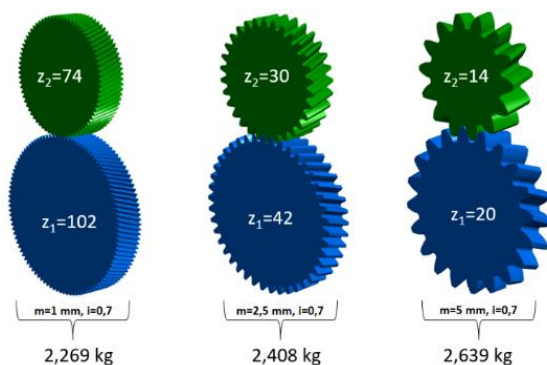


Fig. 44. Gear pair weight according to module

The tooth bending stress, tooth contact stress and safety factor of pinion gears for each speed, which were optimised via KISSsoft, were also calculated according to the mathematical model in ISO 6336. The characteristics of the pinion gears from both KISSsoft and the mathematical model are shown in Tab. 20.

Tab. 20. Optimisation results

Optimisation results	1. Pinion	2. Pinion	3. Pinion	4. Pinion
Tooth-root stress σ_F from KISSsoft (N/mm^2)	543.96	569.46	576.47	570.03
Tooth-root stress σ_F from mathematical model (N/mm^2)	546.97	607.52	625.93	561.37
Safety factor for bending stress S_F from KISSsoft	1.41	1.34	1.32	1.34
Safety factor for bending stress S_F from mathematical model	1.46	1.32	1.28	1.43
Contact stress σ_H from KISSsoft (N/mm^2)	1,363.60	1,286.05	1,292.8	1,197.23
Contact stress σ_H from mathematical model (N/mm^2)	1,345.09	1,264.66	1,239.2	1,226.15
Safety factor for contact stress S_H from KISSsoft	1.10	1.13	1.13	1.22
Safety factor for contact stress S_H from mathematical model	1.12	1.19	1.21	1.22

In Tab. 20, the tooth-root stress of pinion 1 is 546.97 N/mm^2 according to the mathematical model, which is 0.5% larger than the KISSsoft result (543.96 N/mm^2). For the root-safety factor, the results of the mathematical model are 1.46% and 3.5% larger than the results of KISSsoft (1.41). The tooth contact stress of pinion 1 is 1345.09 N/mm^2 according to the mathematical model, which is 1.4% smaller than the results of KISSsoft (1363.60 N/mm^2). For the flank safety factor, the mathematical model result is 1.12 (1.8% larger) than the KISSsoft result (1.10).

For pinion 2, the mathematical model result is 6.7% larger than the KISSsoft result for tooth-root stress. The tooth contact stress according to the mathematical model is 1.7% smaller than the KISSsoft result. For the root-safety factor, the mathematical model result is 1.5% smaller than the KISSsoft result, and the flank safety factor calculated by the mathematical model is 5.3% larger than the KISSsoft result.

For pinion 3, the tooth-root stress according to the mathematical model is 8.5% larger, and the tooth contact stress according to the mathematical model is 4.1% smaller. For the root-safety factor, the result of the mathematical model is 3% smaller, and the flank safety factor for the KISSsoft result is 7% smaller than that of the mathematical model.

For pinion 4, the tooth-root stress according to the mathematical model is 1.5% smaller, and the tooth contact stress is 2.4% larger than the KISSsoft result. The root-safety factor of the mathematical model is 6.7% larger than the KISSsoft result, and the flank safety factors are the same.

According to the results, there is a maximum 8.5% difference between the KISSsoft and mathematical model results ($\sigma_F = 625.93 \text{ N/mm}^2$ by mathematical model and $\sigma_F = 576.47 \text{ N/mm}^2$ by KISSsoft) since KISSsoft considers the tolerances and deformation of gears, and KISSsoft specifies correction coefficients based on user inputs. Although there are some differences between the results, the safety factors calculated using both methods are suitable based on the target values. Therefore, KISSsoft can be used reliably to calculate the strength of gears.

This study is not an improvement study of any design. It is an original work, and therefore there are no pre-existing values with which to compare the results obtained.

6. CONCLUSION

Four speed gears in a tractor transmission were optimised using KISSsoft software. During optimisation, the input power torque, ratios and maximum volume were considered constraints, and the face width, centre distance, module, quality, number of teeth, helix angle, addendum modification coefficient and pressure angle of gear pairs were specified as inputs for the optimisation according to a flow chart. Then, the tooth-root stress, tooth contact stress and safety factors were calculated according to the mathematical model described in ISO 6336. Results were then compared. Regarding tooth-root stresses, the maximum difference was 8.5% for pinion 3. Regarding tooth contact stresses, the maximum difference was 4.1% for pinion 3. Regarding root-safety factors, the maximum difference was 6.7% for pinion 4. Regarding the flank safety factors, the maximum difference was 7% for pinion 3.

According to this study, both the KISSsoft software's results and the mathematical model's results are within the range of the target value. Additionally, the following results were determined via optimisation:

1. Increasing the module increases the root-safety factor and decreases the flank safety factor.
2. Increasing the face width of gears increases the flank safety factor.
3. Increasing the gear quality results increases the flank safety factor.
4. Decreasing the module results increases the number of teeth and overlap ratio.
5. Decreasing the module results increases the sensitivity of the ratio, which can be chosen for the gear pair.
6. Increasing the centre distance decreases the tooth contact stress.
7. Increasing the helix angle increases the contact ratio and axial forces.
8. Increasing the addendum modification coefficient increases the root-safety factor by increasing the tooth thickness.
9. Increasing the addendum modification coefficient decreases the contact ratio.
10. Increasing the module increases the weight of a gear pair.
11. Increasing the pressure angle increases the tooth thickness at the root zone and decreases the tooth thickness at the tip zone.

Optimised gears with other drivetrain components like shafts, bearings, washers, circlip, synchronmeshes are presented as a concept design in Fig. 45-46.

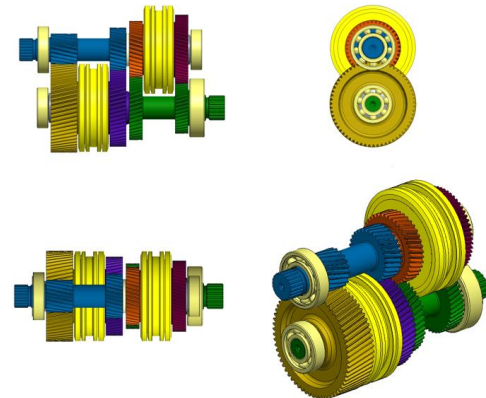


Fig. 45. Concept design

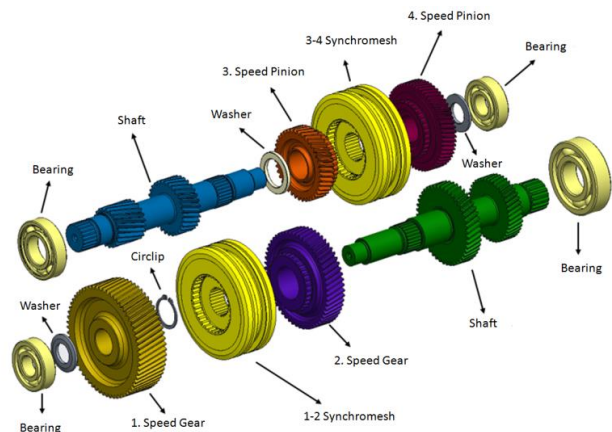


Fig. 46. Disassembly of concept design

The results obtained from this study will be especially beneficial to engineers working in the industry. This is because, in this study, it has been revealed that optimisation serves as a useful tool in the design phase, in which the capability is available to simultaneously and accurately optimise several parameters.

REFERENCES

1. Hlwan HHS, Htay HW, Myint T. Design and contact stress analysis of helical gear for light-weight car. Proceedings of 105th The IIER International Conference. Bangkok, Thailand. 5th – 6th June 2017.
2. Wenkatesh B, Prabhakar SV, Deva PS, Investigate the combined effect of gear ratio, helix angle, facewidth and module on bending and compressive stress of steel alloy helical gear. 3rd International Conference on Materials Processing and Characterisation. 2014;6: 1865-1870.
3. James K, John K. Effect of gear design variables on the dynamic stress of multistage gears. Innovative Systems Design and Engineering. 2012;2:30-42.
4. Murali MV, Ajit SL. Influence of module and pressure angle on contact stresses in spur gears. International Journal of Mechanical Engineering and Robotics Research. 2016;3:224-228.
5. Dyaneshwar S, Mangrulkar KS. Effect of backlash on bending stresses in spur Gears. International Journal of Scientific Development and Research. 2016;7:349-354.

6. Zvonko S, Mileta R, Bozidar R, Dragan R, Zivoslav A. The influence of gear parameters on the surface durability of gear flanks. *Strojarstvo*. 2011;53(5):383-387.
7. Nijazi I, Sadullah A. The influence of sliding speed and specific sliding of the interval meshing gears. 10th International Research/Expert Conference Trends in the Development of Machinery and Associated Technology. Barcelona, Spain, 11-15 September 2006.
8. Karadere G, Yilmaz I. Investigation of the effects of profile shift in helical gear mechanisms with analytical and numerical methods. *World Journal of Mechanics*. 2018;8:200-209.
9. Mujammil A, Mushtaq AC. Optimization of addendum modification for bending strength of involute spur gear. *International Engineering Research Journal*. 2015;1093-1097.
10. Vishal S. Finite element analysis of helical gear pair for bending and contact stresses. *International Journal of Computer Engineering in Research Trends*. 2018;5:136-140.
11. Bozca M, Dikmen F. Optimisation of geometric parameters of ears under variable loading condition. *Advanced Materials Research*. 2012;1005-1010.
12. Bozca M. Optimisation of effective design parameters for an automotive transmission gearbox to reduce tooth bending stress. *Modern Mechanical Engineering*. 2017;7:35-36.
13. Bozca M, Fietkau P. Empirical model based optimization of gearbox geometric design parameters to reduce rattle noise in an automotive transmission. *Mechanism and Machine Theory*. 2010;1599-1612.
14. Bozca M. Torsional vibration model based optimization of gearbox geometric design parameters to reduce rattle noise in an automotive transmission. *Mechanism and Machine Theory*. 2010;1583-1598.
15. Bozca M. Transmission error model-based optimisation of the geometric design parameters of an automotive transmission gearbox to reduce gear-rattle noise. *Applied Acoustics*. 2017;247-259.
16. ISO 6336-3: calculation of load capacity of spur and helical gears, part 3: calculation of tooth bending strength.
17. ISO 6336-2: calculation of load capacity of spur and helical gears, part 2: calculation of surface durability (pitting).

Acknowledgements: This work was supported by Research Fund of the Yildiz Technical University (BAP) Project Number: FYL-2018-3506.

Emre Can:  <https://orcid.org/0000-0002-9298-2616>

Mehmet Bozca:  <https://orcid.org/0000-0002-2620-6053>